P-27

SAN DIEGO SEMICONDUCTORS, INC.

7408 Trade Street
San Diego, California 92121
619/549-4645

POSITION-SENSITIVE CdTe DETECTOR USING IMPROVED CRYSTAL GROWTH METHOD

FINAL REPORT

CONTRACT NO. NAS5-30289

Submitted To

NASA/Goddard Space Flight Center
Greenbelt Road
Greenbelt, Maryland 20771

(NASA-CR-183427) POSITION-SENSITIVE CdTe DETECTOR USING IMPROVED CRYSTAL GROWTH METHOD Final Report (San Diego Semiconductors) 27 p CSCL 20L

N89-25051

Unclas
G3/76 0165853

POSITION-SENSITIVE CdTe DETECTOR USING IMPROVED CRYSTAL GROWTH METHOD

Final Report

Contract No. NAS5-30289

Submitted To

NATIONAL AERONAUTICS AND SPACE ADMINISTRATION
Goddard Space Flight Center
Greenbelt Road
Greenbelt, Maryland 20771

by

San Diego Semiconductors, Inc.
7408 Trade Street
San Diego, California 92121

TABLE OF CONTENTS

SECTION 1

INTRODUCTION

The goal of this program was to demonstrate the feasibility of developing a position-sensitive CdTe detector array for astronomical observations in the hard X-ray, soft gamma-ray region. In principle, it should be possible to improve the resolution capability for imaging measurements in this region by orders of magnitude over what is now possible through the use of CdTe detector arrays. The primary Phase I objective was to show that CdTe crystals of the quality, size and uniformity required for this application can be obtained with a new high pressure growth technique. The approach was to fabricate, characterize and analyze a 100 element square array and several single-element detectors using crystals from the new growth process.

Phase I results showed that detectors fabricated from transversely sliced, 7-cm diameter wafers of CdTe exhibit efficient counting capability and a high degree of uniformity over their entire areas. A 100-element square array of 1-mm^2 detectors was successfully fabricated and operated. Thus, the primary Phase I program objective was met.

SECTION 2

BACKGROUND

2.1 NEED FOR IMAGING TELESCOPES IN X- AND GAMMA-RAY ASTRONOMY

The observation of X- and gamma-radiation from space comprises an important and rapidly growing branch of astronomy that is providing new information about fundamental processes in the universe. As this new discipline has evolved, much more sensitive instruments have been flown in space and from high altitudes. The density of X-ray sources now exceeds one per square degree and one can expect a similar density of high energy X-ray and soft gamma ray sources during the next decade as new instruments come on line. Thus it is necessary to develop techniques for spatially discriminating the incoming radiation with increasingly improved resolution, i.e., much less than one degree. The problem of fabricating less than one degree collimators and the practical need to obtain instrument background measurements and observe many objects dictates that imaging observations are required. Examples of areas under study which will benefit from these improvements include the following:

The Galatic Center Region. Observations of the galactic plane have shown intense, time variable emission from the vicinity of the galactic center. However, spatial resolution limits of the order of 15^{o} for these studies could not differentiate among the many candidate objects, which number in the hundreds, and are separated by as little as a few arc minutes. High energy X-ray and soft gamma-ray imaging observations with arc minute resolution would associate this emission with known optical, radio and IR sources and provide crucial information on the nature of the galactic nucleus itself, e.g., what part of this emission comes from the galactic neucleus and to how high an energy are particles accelerated, and is this evidence for a massive black hole at the galactic nucleus?

Galatic Sources. The locations of many X-ray sources are known to an accuracy of less than one arc minute. However, high energy X-ray and soft gamma ray studies of them, in particular the fainter ones, are hindered by their high spatial density, which is much greater than one per square degree in many regions. Thus, high angular resolution imaging observations are required for the continuing study of galactic sources.

The Extragalactic Gamma-Ray Sky. The cosmic gamma-ray background is generally described in terms of a diffuse component along with a number of detected discrete sources, e.g., quasars and active galaxies and clusters of galaxies. (1). The degree to which the diffuse background itself actually results from the superposed emission of many localized sources is an unresolved and important question that could be fruitfully addressed by spatially resolved, high sensitivity measurements of high energy X-rays and soft gamma rays. The residual, truly diffuse background must come from some unknown intergalactic process or be associated with processes in the early universe, before the period of galaxy formation. Either possibility would have a profound impact on astrophysics. Furthermore, detailed observations of known extra-galactic sources in this energy range should provide valuable insight into the energy processes of these powerful objects (2).

Solar Observations. Imaging of hard X-ray and gamma-ray emissions from solar flares should yield information about important solar phenomena (3).

These emissions are thought to result from the Brehmsstrahlung radiation of decelerating electrons and nuclear interactions of the nonthermal ion component with ambient solar material. Observations of the time evolution of the spatial pattern of such emission should provide important new insight into solar flares hence into fundamental solar processes. In particular, it should be possible to verify current theoretical ideas, i.e., that the nonthermal radiation occurs at the foot of magnetic loops, and to distinguish between competing hypotheses for the sites of the Bremsstrahlung radiation which are the tops of magnetic loops and the bottoms of magnetic loops. The spatial scale of magnetic loops would result in tens of arc seconds of displacement of these sites.

2.2 SYSTEM CONSIDERATIONS

Until recently, it has been difficult to achieve good spatial resolution in the energy range between about 20 KeV and 30MeV. At lower energies, grazing incidence techniques are highly successful(4), while spark gap approaches achieve good resolution at higher energies (5). In recent years the range between 20 KeV and 2 MeV has been addressed through approaches exemplified by the SIGMA telescope (6), using a coded aperture mask in conjunction with a position sensitive detector. The angular resolution is then determined essentially by the ratio of the effective linear dimensions of a detector element to the distance between the detector and the mask.

The basic ideas of the coded aperture technique were first proposed by Dicke (7), and involve the use of a mask with randomly situated open elements. Each such element acts as an individual pinhole camera to produce an image of the source on the detector. The resulting multiple-image pattern is reconstructed to form a single image. This approach maintains the angular resolution of a pinhole camera, with a signal loss of only about 50%. Use of a class of mask patterns based on cyclic difference sets (uniformily redundant arrays) eliminates certain noise and ghosting problems in the original concept (8).

NASA's planned X-Ray Timing Explorer, scheduled for 1993, employs an Anger camera configuration as its position sensitive detector, and is expected to have an angular resolution of about 1^{o}. The Anger camera introduces a number of inherent distortions (9) which can lead to significant positional inaccuracies. An array of individual scintillator/PM tube detectors eliminates these distortions at the expense of larger effective detector dimensions, hence poorer resolution.

A conceptually superior approach to position sensitive detection is to use a planar array of semiconductor detectors. Semiconductor processing techniques can be employed to achieve very small element dimensions and there is no necessity for collecting and detecting a light output. A detector element area of $1mm^2$ should result in an angular resolution of 3.5 arc-minutes for a 2-meter detector-collimator distance. In the future it should be possible to reduce the detector dimensions by at least a factor of ten.

CdTe is believed to be the appropriate semiconductor for balloon and space flight experiments because of its high atomic number and room temperature operation. HqI_2 has similar features, but possesses severe technological problems and requires very high operating voltages. Si and Ge have attractive features, but generally require cryogenic cooling for bulk detectors. Results of the present program demonstrate that our newer crystal growth process makes it possible to obtain large homogeneous crystals of CdTe with the high resistivity and mobility-lifetime product required for detector applications.

SECTION 3

EXPERIMENTAL PROCEDURES AND RESULTS

3.1 OVERVIEW

The experimental portion of this effort included the major task areas of materials processing, device fabrication and device characterization. These subjects are addressed in order in the following subsections.

3.2 MATERIALS PROCESSING

3.2.1 Crystal Growth

It was a major goal of the program to demonstrate that CdTe crystals grown by our new SDS Process possess the high quality and uniformity required in the fabrication of a detector array suitable for astronomical observations. The SDS Process, developed by the program's Principal Investigator, utilizes a variant of the vertical Bridgman technique in a high pressure furnace. The high pressure capability provides a number of distinct advantages for crystal growth in general and for the growth of II-VI compound crystals in particular. Many of these advantages stem from the elimination of quartz from the growth process, made possible by high pressure containment. Quartz is an unavoidable source of a variety of impurities, most notably, oxygen. Such impurities generally reduce carrier lifetimes in CdTe-type materials. In addition, it is believed that oxygen plays a role in the adhesion of the growing crystal to the growth container walls, which causes severe internal strains in the crystal.

The higher temperatures and pressures of over 100 atmospheres attainable with the SDS Process make it possible to optimize temperature gradients and otherwise improve growth conditions to a degree not achievable with conventional quartz-based growth systems. This factor is particularly important for the growth of II-VI compounds because of their tendency toward lattice instability.

Another problem with quartz systems is that they are generally limited in size because of the difficulty in processing the thick walled tubes needed for larger diameter crystals. The 5.0-cm diameter crystals available from present commercial sources probably represent the largest practically attainable from quartz systems. The SDS Process, by contrast, is compatible with substantially larger volumes. Our present furnace is designed for growing CdTe crystals of

up to 7.1-cm in diameter, the actual crystal size and shape being determined by the design of the internal growth crucible. We are assembling a furnace for 12.5-cm diameter crystals, which will be needed for large arrays planned for the future.

The elemental Cd and Te for this program were of quadruple-zone refined grade, available from Cominco Electronics and other suppliers. The Cd and Te were weighed out to provide a composition slightly on the Te rich side of stoichiometry. The raw materials were thoroughly cleaned and acid-etched before they were inserted in a growth crucible.

All detectors and detector arrays reported on in this report were fabricated from two boules, designated as X-08 and X-11. An important aspect of the program was to investigate response uniformity for detectors obtained from various parts of each boule.

3.2.2 Wafer Processing

Wafers were sliced from the boule using our XB-110 band slicer, especially developed for low-damage cutting of materials such as CdTe. The wafers were lapped to final thickness using a SiC grit slurry, with grit size being progressively reduced from 12 μm to 0.3 μm, then were subjected to a final free etch to remove surface damage.

Portions of the wafers were routinely characterized with respect to resistivity, etch pit density and gamma ray sensitivity, and visually inspected for quality of crystallinity. For resistivity and gamma ray sensitivity measurements, a series of 1-mm diameter contact pads was deposited around the circumference and within the central region of every wafer evaluated; this approach provided an assessment of the uniformity of critical generating parameters. Selected samples were sent to an outside service for X-ray rocking curve studies of crystallinity.

The following general observations can be made about characterization results:

a. resistivities were 10^9 ohm-cm or higher over more than 70% of both boules X-08 and X-11; and were remarkably uniform from center to circumference in the high resistivity section;

b. the uniformity of gamma-ray sensitivity was comparable to that of resistivity;

c. etch-pit densities were in the low 10 cm- range over most of both boules;

d. it was possible to obtain single-crystalline, twin-free surfaces with good crystallinity over areas greater than 10 cm ;

e. there was no apparent correlation between crystalline quality and sensitivity to gamma radiation.

3.2.3 Wafer Metallization

The basic detector structure consists of a CdTe wafer with its opposing broad area surfaces metallized in such a way that the contact is nonrectifying. Reported instances of polarization (10) and certain other problems appear to be related to band bending in the semiconductor caused by improper contacting materials. Our contacting materials were perfected over several years and involve a number of critical steps. We do not observe polarization effects.

3.3 DEVICE DESIGN AND FABRICATION

3.3.1 Single Element Detectors

Areas of single-element detectors were defined by using the XB-110 Crystal Slicer to cut wafers transversely to their broad area faces, after metallization. Detector thickness, established in the wafer processing stage, was chosen on the basis of the following considerations.

The dependence of count rate on voltage for CdTe can be expressed as (11)

$$N = \frac{N_o}{2} \operatorname{erfc}\left[\frac{\tau}{\Delta\tau}\left(\frac{V_o}{V} - 1\right)\right] \qquad (1)$$

where τ is the ensemble average electron lifetime, is the spread in average lifetimes due to crystalline inhomogeneities or other factors, N is maximum attainable (saturation) count rate and V is the voltage at which $N = 0.5N_o$. It can be shown that

$$V_o = \frac{E_m L^2}{\mu_e V E} \qquad (2)$$

where L is the detector thickness, μ_e the electron mobility, E the gamma quantum energy and E_m the energy equivalent of the minimum charge detectable by the electronic system employed.

Equation 1 shows that, in principle, the saturation count rate level can always be approached by making V large enough. In practice, V is generally limited by surface-related noise effects. The goal of detector development, then, is to minimize V_o for an acceptable count rate.

Equation (2) shows that, with all else held constant, V_o is strongly dependent on L, which should be minimized. Off-setting this consideration is the necessity that L be large enough for efficient absorption of gamma rays (i.e., V_o increases with L). A third factor is the expected range of gamma quantum energies, which relates to performance as indicated in Eq. 2 and through the energy dependence of the absorption coefficent.

From consideration of the above factors and the various trade-offs involved, it was determined that an optimum thickness for detectors in this study should be in the range of 1.0 - 1.5 mm. A specific value of 1.2 mm was chosen.

Detectors from Boules X-08 and X-11 were fabricated specifically for this program and were subjected to detailed characterization and analysis.

Boule X-11 was also used in the fabrication of commercial detectors, which are standard products of this company. A survey of the performance of commercial detectors provides information on the overall uniformity of the boule and was included in the program. Results of these efforts are presented and discussed in Section 3.5, below.

3.3.2 Detector Array Fabrication

The approach to array fabrication for this program was, in essence, to fabricate a very large detector (1.4X1.4 cm^2, approximately), then score one surface into the desired array

pattern using the XB-110 slicing saw. The objective was to produce a square array of 100 $1mm^2$ detector elements. The bottom surface then consisted of a completely metallized plane. A number of preliminary cuts were made on graphite wafers and scrap CdTe material. The final cuts were made on a metallized wafer from a Boule X-11 sample which had been evaluated to assure that it performed as a detector. The final cut surface is shown in Figure 3-1.

A number of unexpected difficulties were encountered with this approach. In the first place, it was discovered that the contact metallization process actually produces a low resistivity region below the metal layer, 10 - 50 μm in depth. In order to isolate the individual elements, it was necessary to cut through this region. Thus, instead of simply scoring a thin metal layer, it became necessary to cut into the crystal to a significant depth.

Then, it is a normal action of the cutting process to cause microchipping at the entry surface of a crystal. In the usual wafer slicing operation, microchipping is a neglible feature. With small element areas, however, the jagged edges caused by microchipping resulted in a serious loss in area definition. The jagged edges are clearly evident in Fig. 3-1. The microchipping is also believed to have caused some internal lattice damage and consequent loss in detector sensitivity.

The microchipping problem is believed to be related to small, resonant vibrations in the rotating saw blade. We were able to significantly reduce, but not eliminate the effect, by adjusting blade tension and redesigning certain portions of the fixture. We believe the effect would be eliminated by using a blade with reciprocating motion, as is utilized on certain multi-wafer wire saws. However, as will be discussed in Sections 4 and 5, we believe the best approach to further array fabrication would be to use photoresist masking to form the metallized pattern and eliminate the sawing operation altogether.

3.4 DEVICE CHARACTERIZATION

3.4.1 Single Detectors

The essential parameters to be investigated were count rate, energy resolving capability, and noise. The general approach was to measure these quantities as functions of bias voltage, and attempt to correlate results with recent theoretical developments. Detectors fabricated from wafers obtained from various portions of Boules X-08 and X-11 were characterized.

ORIGINAL PAGE
BLACK AND WHITE PHOTOGRAPH

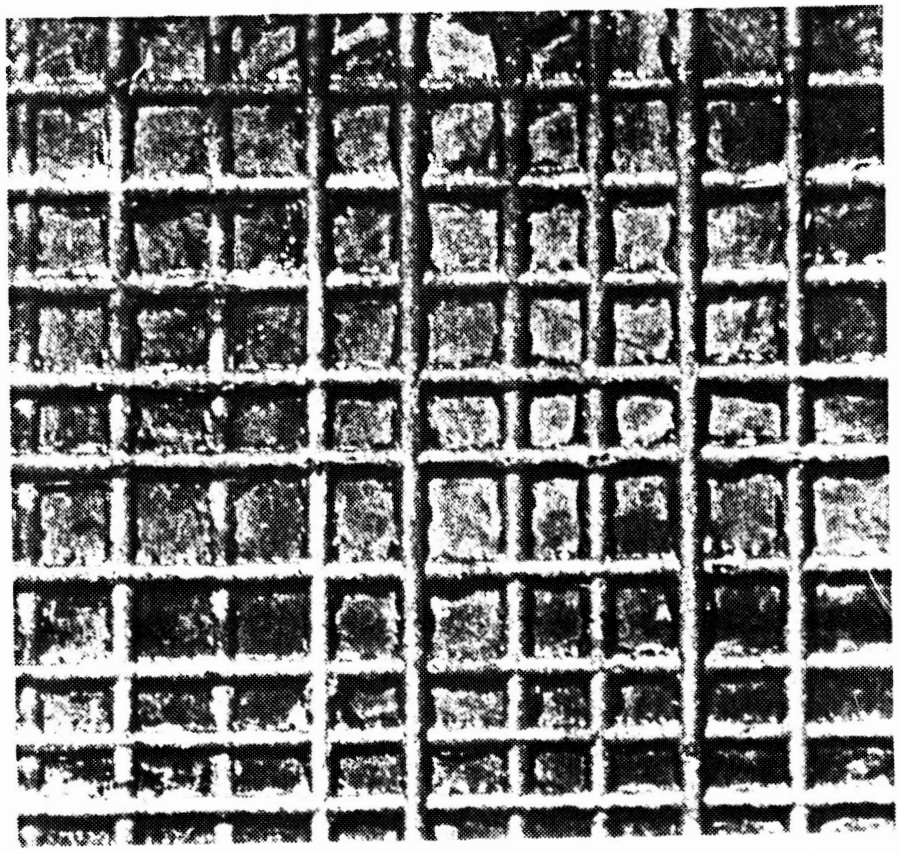

FIGURE 3-1

CdTe DETECTOR ARRAY
NOMINAL ELEMENT AREA = 1 MM

Detectors investigated included three devices assembled specifically for this program and more than ten detectors produced for commercial sales.

Figure 3-2 shows typical results for count rate as a function of bias voltage for a single element detector. The data were obtained using low intensity ("license-free") radioactive sources situated approximately 2 mm from the detector surfaces. The maximum count rates for this configuration are typically in the order of 10^4 c/s or larger. Previous studies (12) have shown that the count rate is linear with gamma ray flux from background to levels in excess of those employed in these studies. In Figure 3-2, the solid points represent experimental values, while the curves were generated from Eq. 3-1, using curve fitting techniques. The curves were fit to the data using $\Delta\tau/\tau = 0.67$. The experimental values were normalized to the saturation level of each quantum energy. The saturation levels inferred from the curve-fitting process agree with the photon absorption rate as calculated from the relation

$$R = \phi A[1 - \exp(-\alpha L)] \qquad (3)$$

where ϕ is the photon flux incident on the detector surface, A the detector area and α the absorption coefficient.

Curves such as those in Figure 3-1 are useful in comparing detectors. For example, for a given energy, Eq. 3-2 shows that V_o is inversely proportional to the mobility-lifetime product. Comparison of V_o from one detector to another thus provides an effective method of evaluating the relative performance of different detectors in an array, or of detectors obtained from different reqions of a crystal. Six detectors fabricated from various sections of a single transverse wafer from boule X-11 showed no variation in the mobility-lifetime within experimental error. The performance of four detectors fabricated from a wafer oriented along the growth direction indicated that a gradual decrease in mobility-lifetime in going from the first-to-freeze to last-to-freeze regions. The total decrease was approximately 15%.

The upper limit on bias voltage in the studies was established by an excess noise phenomenom in the form of a high counting rate that typically emerged in the 40-100 volt range. The voltage at which this noise became evident could

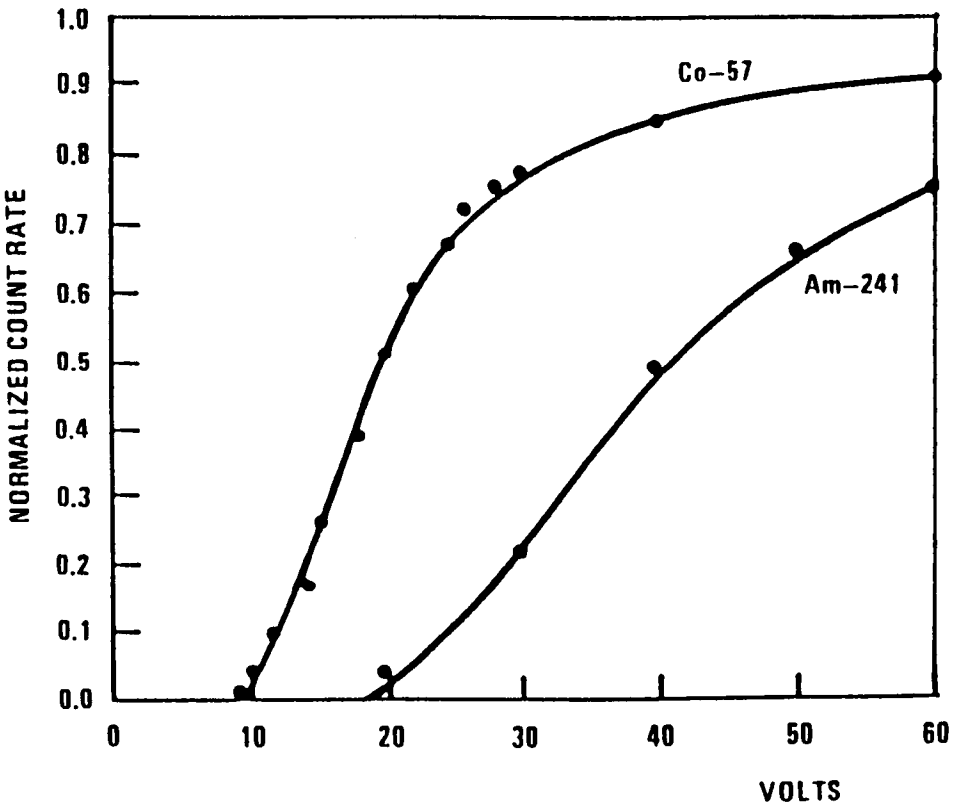

FIGURE 3-2

DEPENDENCE OF COUNT RATE ON BIAS VOLTAGE FOR A TYPICAL CdTe SINGLE ELEMENT DETECTOR. QUANTUM ENERGIES ARE 59.6 KeV FOR Am-241 AND 123 KeV AND 136 KeV FOR Co-57.

generally be increased significantly by surface cleaning operations, hence the effect is believed to be surface-related.

Energy spectra of single-element detectors were measured with a variety of sources. Spectra of detectors are routinely observed on a video display multichannel analyzer, in our laboratory. Selected detectors were evaluated at the laboratories of the University of California, Los Angeles Medical Center. Results for a typical device, kindly made available by Dr. F. Daghighian of that organization, are presented in Figures 3-3, 3-4, 3-5 and 3-6. For conditions of these measures, the resolution E is expected to be in the order of

$$\frac{\Delta E}{E} \simeq \frac{2\Delta\tau}{\tau} \qquad (3-4)$$

The spectral widths in Figs. 3-3, 3-4, 3-5 and 3-6 are consistent with Eqs. 3-4.

3.4.2 Detector Array Characterization

Array characterization made use of a special probing apparatus which allowed contact to be made individually and successively to the array elements. This arrangement made it possible to use a single preamplifier for all detectors. The first-stage FET of the preamplifier was mounted in close proximity to the contacting probe to minimize capacitance. The detector, probe and preamplifier components were all installed in a light-tight metal box. The probe position could be controlled by a 3-axis micrometer arrangement. The gamma-ray sources were contained in sealed, 1-in diameter disks which could be installed on a platform built for this purpose on the probe assembly.

Count rate vs. voltage curves were performed on six array elements. In all cases, results were qualitatively the same as that of Figure 3-2, but quantitative comparisons were not feasible because of area definition problems to be discussed below. Two of the one hundred detectors exhibited short circuits, probably as a result of an inclusion in the crystal lattice structure.

In order to minimize performance differences, the detectors were operated as far up into the saturation region as

FIGURE 3-3

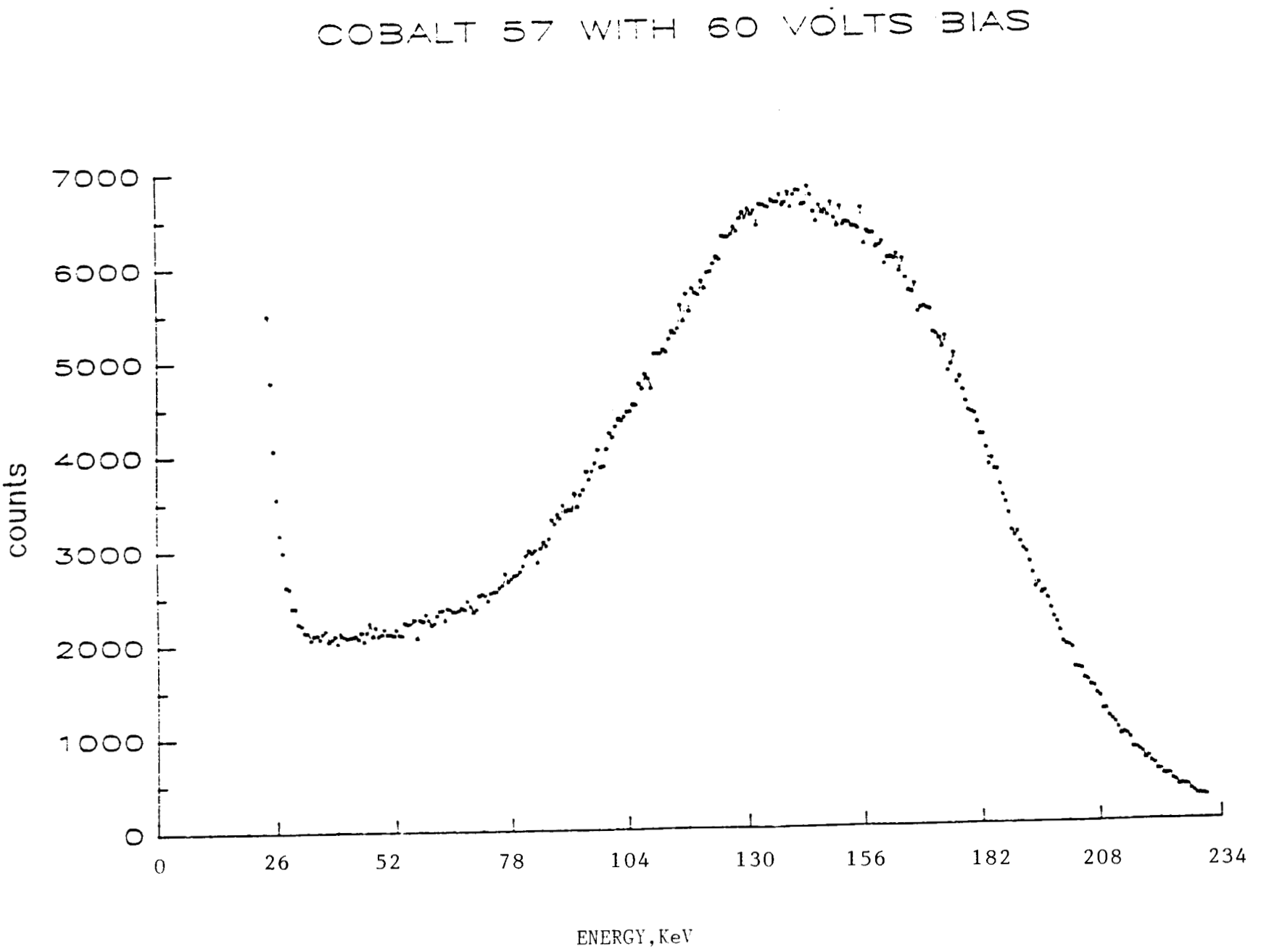
COBALT 57 WITH 60 VOLTS BIAS
counts
7000
6000
5000
4000
3000
2000
1000
0
0
26
52
78
104
130
156
182
208
234
ENERGY, KeV

FIGURE 3-4

INDIUM WITH 60 VOLTS BIAS

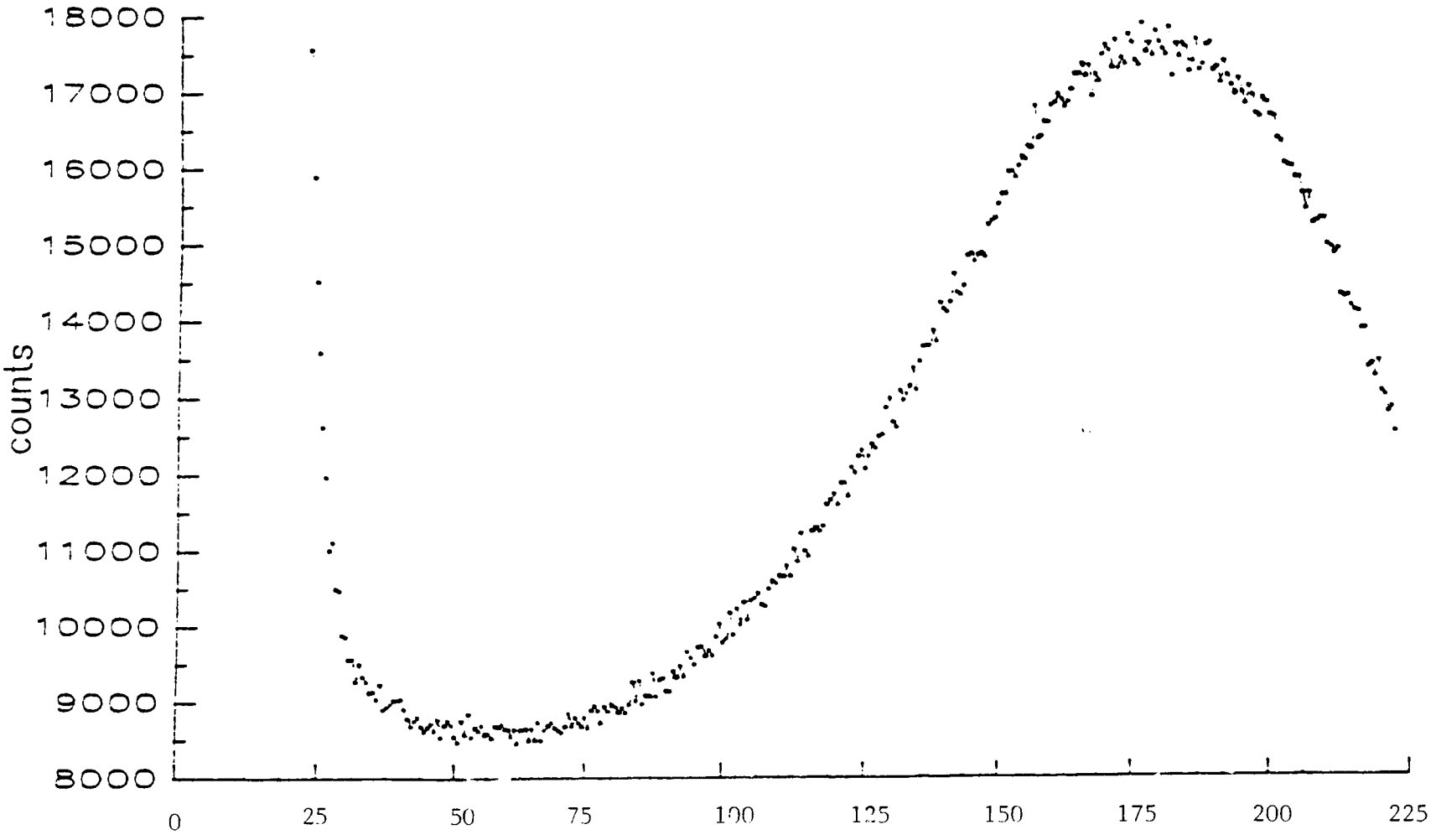

FIGURE 3-5

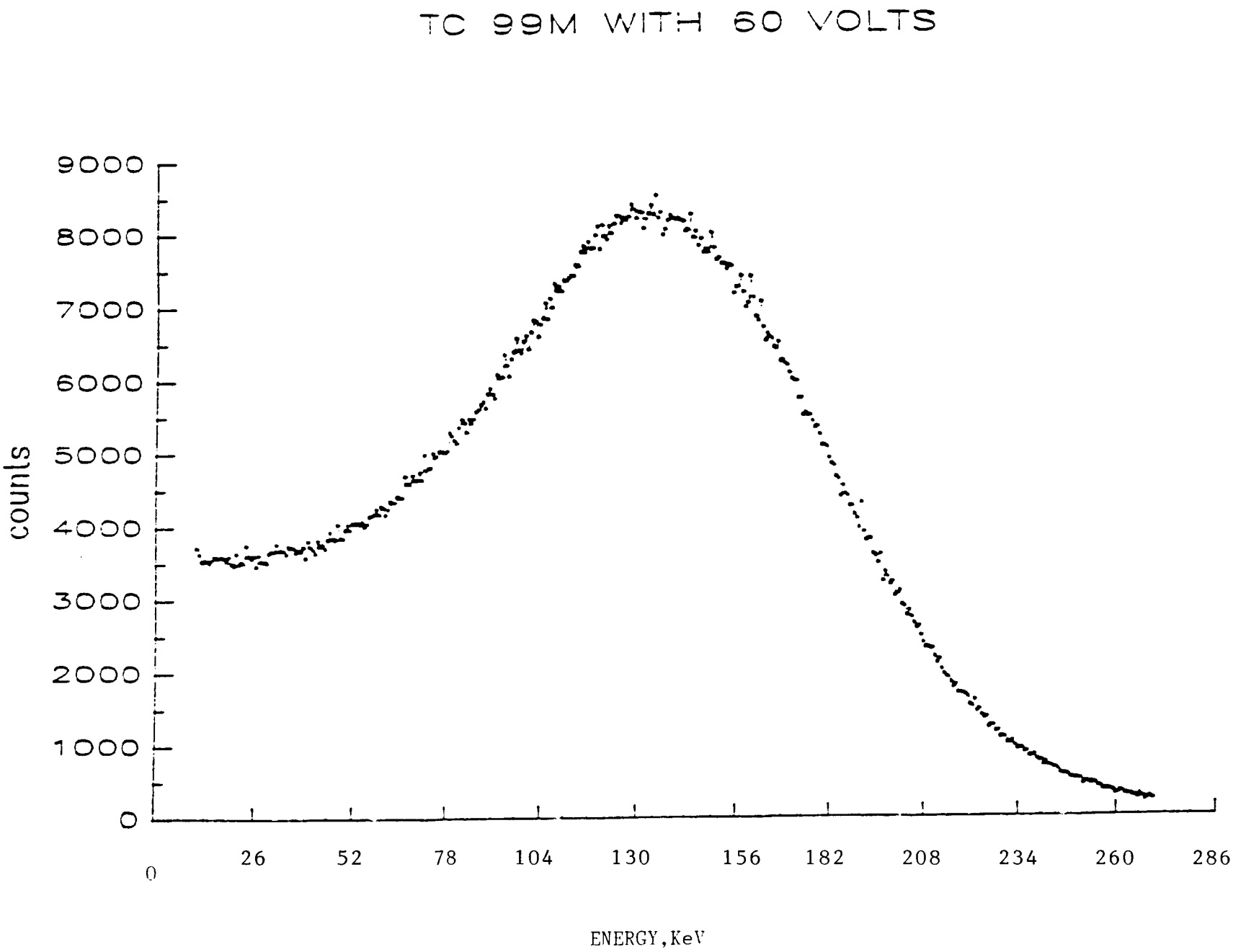
TC 99M WITH 60 VOLTS
counts
9000
8000
7000
6000
5000
4000
3000
2000
1000
0
0
26
52
78
104
130
156
182
208
234
260
286
ENERGY, KeV

FIGURE 3-6

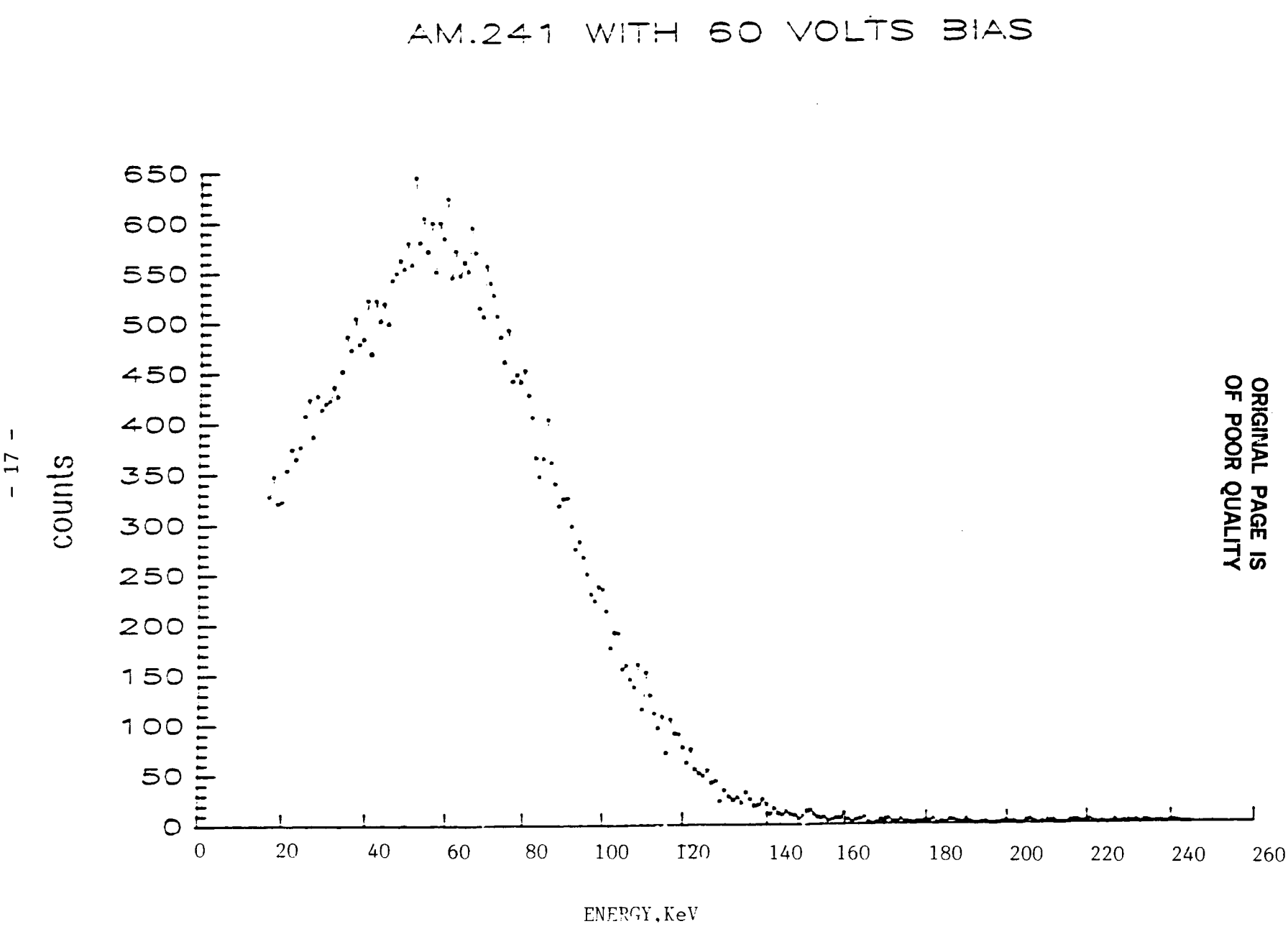

possible. In practice, the bias voltage was limited to 50 volts by excess noise problems discussed previously.

The array was evaluated at 50 volts using three quantum energies, 123 KeV (Co-57), 663 KeV (Cs-137) and 1.2 MeV (Co-60). The approximate incident flux levels on the array were 1800/min/mm^2 for Co-57, 3600/min/mm^2 for Cs-137 and 360/min/mm^2 for Co-60. According to the manufacturer of the radiation sources, the error in source strengths was +/-20%. For reasons to be discussed later in this section, there was a great deal of variability in the counting rates from one element to another. An attempt was made to correct the data for variations in element area by measuring every element area microscopically with a calibrated lens attachment. The count rates were then divided by the respective areas and normalized to an assigned value of 100 for Element #46, situated near the array center. Table 3-I, below gives the theoretical maximum and measured count rates

TABLE 3-I

COUNTING RATE FOR ELEMENT NO. 46
BIAS VOLTAGE = 50 V

Radioactive Source	Theoretical Maximum Rate (C/M)	Measured Maximum Rate (C/M)
Co-57	1800	1600
Cs-137	216	200
Co-60	13	10

for Element #46. The agreement between measured and theoretical values is surprisingly good, in view of the problems in area determination to be discussed.

The count rate data, after correcting for the visually determined areas, are presented in Figs. 3-7, 3-8, and 3-9. It is apparent that the data still exhibit a considerable amount of scatter. We believe the two major sources for the remaining scatter are as discussed in the following.

a. Scatter Due to Microchipping. As shown in Fig. 3-1, the element edges are highly irregular. Closer inspection shows that the edges are fractured in a chonchoidal manner resulting in a gradation of depth away from the metal layers rather than in vertical walls. Since, as discussed earlier, the low resistivity contact region

10 55	9 99	8 97	7 95	6 77	5 131	4 154	3 122	2 149	1 59
20 129	19 143	18 142	17 123	16 141	15 169	14 127	13 149	12 148	11 171
30 123	29 143	28 145	27 155	26 142	25 161	24 151	23 147	22 168	21 206
40 73	39 128	38 135	37 85	36 130	35 110	34 127	33 86	32 132	31 97
50 42	49 124	48 128	47 127	46 100	45 ---	44 ---	43 131	42 153	41 88
60 127	59 139	58 140	57 154	56 121	55 131	54 113	53 153	52 131	51 150
70 62	69 114	68 124	67 138	66 128	65 147	64 107	63 106	62 125	61 173
80 103	79 116	78 136	77 159	76 170	75 136	74 201	73 159	72 151	71 166
90 88	89 104	88 99	87 137	86 108	85 147	84 118	83 94	82 81	81 101
100 110	99 93	98 85	97 93	96 91	95 108	94 96	93 110	92 123	91 109

FIGURE 3-7

CdTe ARRAT DETECTOR PERFORMANCE

Co 57 (E = 122 KeV)

10	9	8	7	6	5	4	3	2	1
.49	85	100	81	87	146	138	155	128	91
20	19	18	17	16	15	14	13	12	11
60	128	140	123	133	146	131	141	137	174
30	29	28	27	26	25	24	23	22	21
111	121	125	133	125	138	130	127	153	148
40	39	38	37	36	35	34	33	32	31
.81	117	122	111	121	138	115	98	123	125
50	49	48	47	46	45	44	43	42	41
75	109	108	113	100	---	---	117	143	70
60	59	58	57	56	55	54	53	52	51
108	128	125	147	115	134	96	133	128	153
70	69	68	67	66	65	64	63	62	61
75	95	105	116	110	133	125	146	114	148
80	79	78	77	76	75	74	73	72	71
89	117	117	134	144	122	168	139	138	155
90	89	88	87	86	85	84	83	82	81
77	92	89	118	98	128	123	103	83	95
100	99	98	97	96	95	94	93	92	91
115	105	113	97	100	113	107	113	117	108

FIGURE 3-8

CdTe ARRAY DETECTOR PERFORMANCE

Cs^{137} (E = 660 KeV)

10 34	9 116	8 108	7 84	6 101	5 124	4 128	3 130	2 122	1 96
20 59	19 109	18 122	17 118	16 112	15 121	14 108	13 122	12 125	11 129
30 87	29 110	28 138	27 117	26 116	25 124	24 121	23 124	22 108	21 130
40 59	39 99	38 101	37 122	36 108	35 124	34 99	33 89	32 108	31 114
50 58	49 97	48 99	47 111	46 100	45 ---	44 ---	43 92	42 125	41 86
60 121	59 108	58 114	57 124	56 105	55 122	54 106	53 112	52 104	51 123
70 49	69 98	68 97	67 115	66 117	65 116	64 117	63 121	62 110	61 124
80 52	79 99	78 118	77 119	76 122	75 110	74 130	73 122	72 122	71 119
90 87	89 90	88 95	87 103	86 90	85 118	84 101	83 93	82 91	81 92
100 102	99 97	98 101	97 95	96 95	95 102	94 96	93 102	92 102	91 101

FIGURE 3-9

CdTe ARRAY DETECTOR PERFORMANCE

Co 60 (E = 1.333 KeV)

actually extends a significant distance below the crystal surface, the graded edges effectively extend the contact areas a significant but indeterminate distance beyond the visible metal layers. Thus, the actual areas are larger than the visually-defined areas, and are not readily ascertainable.

b. Fringing Fields. When a single array element is biased, fringing fields result in detection capability within the crystalline region outside of the metal pad area. Analysis shows that the effective dimensions of an element may be extended by an amount comparable to the detector width by this effect. In an operating array, in which all elements are maintained at the same DC level, the fringing fields largely cancel each other out and become restricted to small regions between the metal pads. Thus, fringing field problems are expected to be very small in an operating array, but to have a large effect in our measurements on single elements of an array structure.

The fringing field problem becomes magnified when the jagged, poorly-defined element edges are considered, because the extent of the fields depend to a large degree on edge configuration. Thus, the combination of poorly determined edge geometry and fringing fields makes the determination of detector active areas virtually impossible. We believe these factors explain the wide variations in the data of Figs. 3-7, 3-8 and 3-9.

Attempts were made to eliminate the microchipping problem by adjusting the tension on the rotating blade of our Model XB-110 slicer. The effect was reduced, but it appeared that small resonant vibrations that appeared to be the source of the problem could not be altogether eliminated. It is believed that a successful approach to eliminating the microchipping problem would be to utilize a saw based on a reciprocating motion rather than the continuous rotating motion now employed.

However, as will be discussed in the next section, it is believed that the use of a photoresist-based process which altogether eliminates the need for sawing offers a superior approach.

SECTION 4

CONCLUSIONS AND RECOMMENDATIONS

Characterization and analysis of single-element detectors obtained from many regions of two separate boules demonstrated that wafers sliced transversely to the growth direction possess the required quality and uniformity for large array applications. Five-inch diameter boules grown in the furnace now under construction should make it possible to achieve single-wafer array areas of over 50 cm^2.

The 100 element square array evaluated in the program has two significant problems. In the first place, the sawing technique used to score the crystal surface caused unavoidable microchipping and consequent loss of area definition. In the second place, a separate preamplifier will be needed for each element in an operating array; for an array of several thousand elements, the interfacing problems will be non-trivial.

We believe a different array configuration will surmount both of these problems. The recommended new approach is to utilize a matrix configuration consisting of metal stripes with transverse orientation (rows and columns) on opposing surfaces of a wafer. One preamplifier will be needed per stripe, and may be attached at a convenient edge location. The stripes can be formed by standard photoresist processing techniques and no sawing or scoring operations are needed. This approach should also make it possible to achieve much smaller element sizes (and consequent better resolution potential) in future arrays.

SECTION 5

REFERENCES

1. F.E. Marshall, et al, Ap.J. v235 4 (1980).

2. R.E. Rothschild, et al, Ap.J. v269 423 (1983).

3. T.A. Prince, et. al, to be published in Solar Physics (1988).

4. L. Scarci, et al, Prol. 12th ESLAB Symposium, Frascati, ESA SP-124, 3.

5. R. Ciacconi, et al, Astrophys. J. 230, 540 (1978).

6. J. Paul, et al, 20th ICRC Conf. 06-9 Session, Moscow (1987).

7. R.H. Dicke, Astrophys. J. V153, L101 (1968).

8. E.E. Fenimore and T.M. Cannon, Appl. Optics, V17, 337 (1978).

9. J.A. Sorenson and M.E. Phelps, "Physics in Nuclear Medicine" (Harcourt Brace Jovanovich, NY, 1987) pp. 318-327.

10. H.L. Malm and M. Martini, IEEE Trans. Nucl. Sci., v 21, 322 (1974); P. Siffert, et al, ibid, v 23, 159 (1976).

11. J.F. Butler, To be published.

12. Final Report, "Improved Performance Nuclear Particle Detector," Department of the Army, EW/RSTA, USACECOM, Ft. Monmouth, NJ 07703, Contract No. DAABO-86-C-P029.